

Original Research Article

Ecological and Economic Feasibility of Inductive Heating for Sustainable Press Hardening Processes

**Florian Pfeifer^{*1}, Lukas Knorr², Florian Schlosser²,
Thomas Tröster¹, Thorsten Marten¹**

¹Automotive Lightweight Design, Paderborn University, Warburger Str. 100, 33098 Paderborn, Germany

e-mail: florian.pfeifer@uni-paderborn.de

²Energy System Technologies, Paderborn University, Warburger Str. 100, 33098 Paderborn, Germany

e-mail: lukas.knorr@uni-paderborn.de

Cite as: Pfeifer, F., Knorr, L., Schlosser, F., Marten, T., Tröster, T., Ecological and Economic Feasibility of Inductive Heating for Sustainable Press Hardening Processes, *J.sustain. dev. energy water environ. syst.*, 11(3), 1110450, 2023, DOI: <https://doi.org/10.13044/j.sdewes.d11.0450>

ABSTRACT

Press hardening is an established process for producing high-strength, lightweight structural automotive parts, utilising roller hearth furnaces to heat metal sheets. It presents a non-negligible source of greenhouse gas emissions in part production processes. This paper investigates the ecological and economic advantages of induction as an alternative heating method and identifies break-even scenarios. Therefore, specific energy demands for various furnace and induction heating operating states are determined and applied to different energy system transition scenarios. It can be shown that while induction heating can be more energy efficient than furnace heating, its ecological and economic advantages are highly dependent on regional electricity-to-gas price ratios and electric energy emission factors. For high good-mass flows (0.5 kg/s) and 80% production capacity utilisation, an electricity-to-gas price ratio lower than 1.24 and an emission factor lower than 250 g_{CO2}/kWh are required.

KEYWORDS

Press hardening, Induction, Decarbonisation, Electrification, Sector coupling, Ecological feasibility, Economic feasibility.

INTRODUCTION

To meet the goals set by the European Union in the European Climate Law (Regulation (EU) 2021/1119), a reduction of greenhouse gas (GHG) emissions by increasing energy efficiency and using sustainable energies is necessary [1]. Both transport and industrial production are responsible for a major share of Europe's GHG emissions. Emissions caused by the transport sector represent almost a quarter of Europe's GHG emissions; it is also the main cause of city pollution [2]. Industrial processes are responsible for about 22% of the overall GHG emissions [3]. A large proportion of these emissions are caused by process heat generation [4]. While emissions at lower temperature levels can already be reduced by heat recovery and electrification using heat pumps [5] or hybrid heat pump-electric boiler systems [6], the technological development for high-temperature applications is significantly lower [7].

Lightweight design is an established method for reducing the fuel consumption of internal combustion engine vehicles in the transport sector. It can help increase electric vehicles' energy

* Corresponding author

efficiency during their use phase [8]. Additionally, it offers various non-energy related advantages, such as increased road user safety, enhanced driving dynamics and reduced particle pollution [9]. The impact of lightweight design on GHG emissions over a vehicle's full life cycle depends on various factors, such as vehicle type and characteristics, as well as manufacturing processes and energy supply of material production [10].

The press hardening of steel sheet components is a fundamental process for producing high-strength lightweight structural parts in the automotive industry, such as A- and B-pillars, door beams, rocker panels or roof reinforcements [11, 12]. The number of press-hardened parts has increased yearly since Saab Automobile AB introduced the process to the automotive industry in 1984 [13]. In 1987, only 3 million parts per year were manufactured through press hardening [14]. In 2017, the number of produced press-hardened parts was estimated to be 300 million per year, with further increases predicted over the coming years [15]. Modern car bodies can include up to 38% of their total body in white weight (i.e., before painting) in press-hardened steel [16].

Press hardening of steel sheets utilises structural transformations of the iron atom lattice during heating and cooling for material hardening. It requires heating the wrought material before it can be formed and quenched in forming tools. On existing manufacturing lines, metal sheets are usually heated in roller hearth furnaces [11, 17]. Long heating times due to convection- and radiation-based heating [11, 18], low flexibility of heating processes [17, 19], high space requirements of those furnaces [14, 20] and low energy efficiency [19] due to high standby demand and high surface heat losses lead to the investigation of alternative heating methods. One promising approach is the heating of sheet metal using induction. Induction heating uses direct thermal energy transfer through electric Joule heat. It can, under certain circumstances, lead to a more time-, space- and energy-efficient heating process for press hardening applications [21, 22].

Additionally, the electric energy-based nature of inductive heating could open up the possibility of a heating process entirely powered by sustainable energies, another advantage of inductive heating over traditional gas-fired conveyor furnaces. It would help mitigate GHG emissions caused by the industrial sector and increase the impact of lightweight design on the GHG emissions over a vehicle's life cycle. The economic and ecological feasibility of such an induction process strongly depends on the price ratio of the competing energy carriers, electricity and natural gas, and the development of the emission factor of the electricity grid. In addition, logistical production conditions like utilisation and good-mass flow affect economic efficiency.

Objective

This study aims to determine the emissions and costs for inductive heating compared to conventional gas-fired roller hearth furnaces for different parameter sets of boundary conditions like product mass flow, utilisation, energy prices and emission factors depending on energy transition scenarios. Based on this evaluation matrix, one can identify break-even conditions that favour inductive heating.

STATE-OF-THE-ART PRESS HARDENING

Press hardening combines the manufacturing methods of deep drawing and hardening [23]. Its advantages are the good formability of heated steel sheets, low springback, good dimensional accuracy and the high strength of parts after forming [11, 24]. Those properties enable the production of automotive structural components with higher strengths than achievable through cold stamping of steel sheets [11]. The possible decrease of sheet metal thickness compared to cold-formed steels allows the reduction of weight in parts where high structural stiffness is desirable [12, 21]. Conventional press hardening processes also have drawbacks compared to cold forming, such as increased process complexity, increased

investment and production costs, higher space requirements and reduced productivity [11]. Therefore, constant research on these topics is necessary to improve the overall process.

The process of press hardening can be divided into two main variants: direct and indirect press hardening [14]. For both variants, steel sheets are first cut from a steel coil. During the direct press hardening, the sheets are heated before being transported to a hydraulic press, quenched in a forming tool, and received final geometry. Afterwards, other processes, such as cutting, surface finishing or joining, may follow. During the indirect press hardening process, an additional cold-forming step is included before heating. It allows manufacturing components of higher complexity while reducing tool wear of the hot forming tool [12, 24]. However, the additional process step and a higher necessary tool application lead to increased part costs, which is why direct press hardening is more commonly used in industrial processes [12]. This study focuses on the direct press hardening process shown in Figure 1.

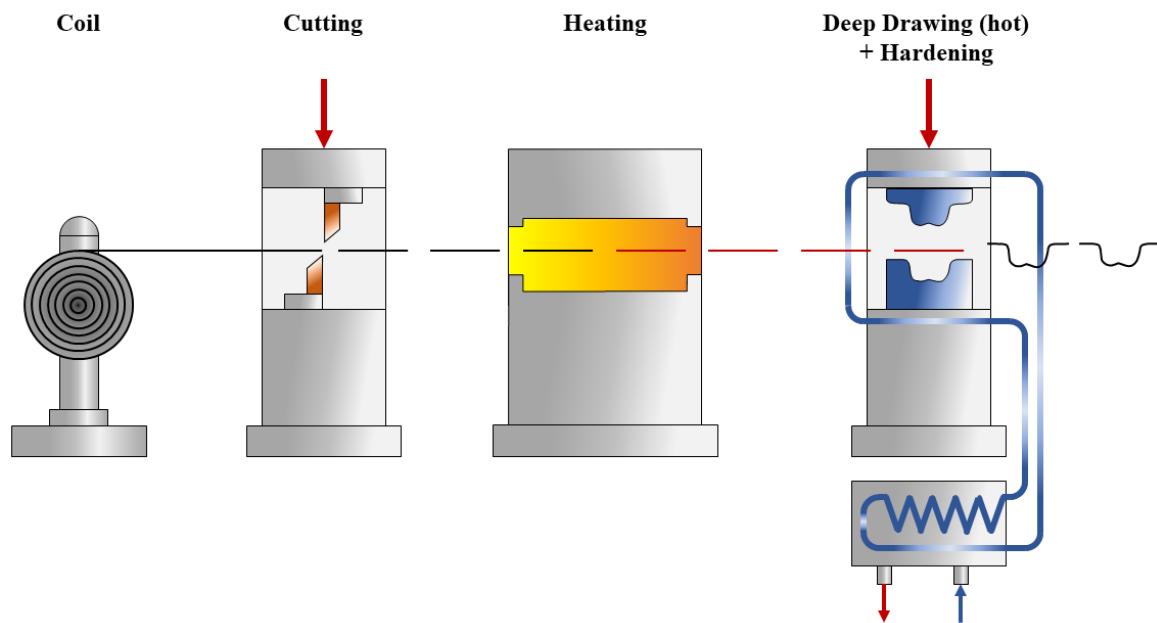


Figure 1. Schematic overview of the direct press hardening process

As mentioned before, temperature-induced transformations of the iron atom lattice are utilised during press hardening to achieve the high strength of manufactured components. For materials used in industrial press hardening processes, temperatures of 900 °C to 950 °C with furnace dwell times of several minutes are common, and a cooling rate of more than 25 K/s is sufficient for forming a high-strength martensitic structure [11, 14, 24]. Low-alloy boron-manganese steels are typically applied for industrial press hardening [12]. The alloying elements boron and manganese positively influence the alloyed steel's hardenability and required cooling rates and increase the attainable material strength [12, 24]. Of the available boron-manganese steels, the steel 22MnB5 is the most commonly used [11, 12, 14]. After hardening, this steel reaches a tensile strength of approximately 1500 MPa and an elongation at fracture of approximately 5% [25].

Conventional roller hearth furnaces used for press hardening are heated through gas combustion or electricity [11, 18, 19]. An average of 21.3% of the combustion energy of natural gas is lost as waste heat in the form of exhaust gases [19]. By applying, for example, an absorption chiller based on the waste heat, one can recover a maximum of 69% of this heat for press cooling. In addition, diffuse heat losses occur depending on the furnace geometry and design of at least 54% over the large surface of the roller hearth furnaces, irrespective of the material mass flow conveyed. Heat is transferred to the steel sheet through radiation and convection, leading to long heating times of several minutes [11, 18, 20, 21]. However, the typical press hardening cycle takes approximately 20 s to 30 s [11, 21]. Therefore, to meet the

good-mass flow requirements of the process press cycle, conventional roller hearth furnaces need to be designed with sufficient dimensions and can reach a length of up to 40 m, resulting in high space requirements [11, 20, 21].

Additionally, due to the long times needed to heat up or cool down roller hearth furnaces, furnaces often are continuously heated, even when part production is stopped, for example, because of maintenance or production errors [17, 19]. It leads to high energy demands even in no value-adding times. Various alternative heating methods have been investigated based on these disadvantages of conventional furnaces heating.

Alternative heating concepts for press hardening

One driving factor for the investigation of alternative heating methods is the desire for increased heating rates of sheet metal. Therefore, research has been conducted on various heating technologies and their application for press hardening. These technologies involve, but are not limited to, infrared heating [26, 27], induction heating [18, 22, 28, 29], resistance heating [30–33], contact heating [34–37], fluid bed heating [38] and direct flame heating [39]. While all these technologies have advantages and disadvantages, the current study focuses on applying induction heating. An oscillating magnetic field is created during induction heating by an induction coil, the so-called inductor. If an electroconductive material enters the magnetic field, an electric current is induced into the material, leading to increased material temperature through the effects of Joule heating. The advantages of induction heating, compared to conventional furnace processes, are high achievable heating rates, low space requirements and high energy efficiency in terms of less surface heat losses and no standby heat demand [20, 21]. Challenges of inductive heating are the homogeneity of heating [18, 22, 28] and resulting material and coatings properties [40, 41]. According to Kolleck *et al.*, inductor arrangements for sheet metal heating can be divided into three major categories, shown in Figure 2 [42].

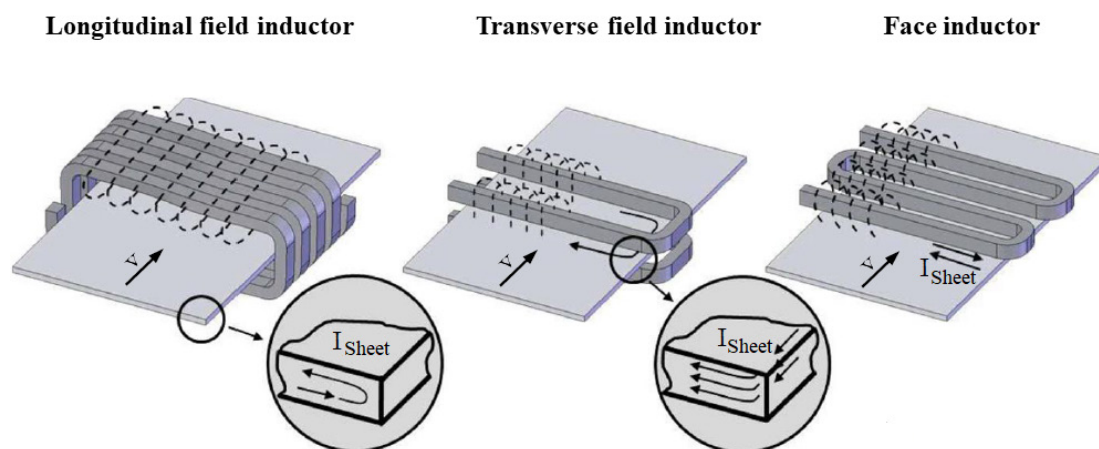


Figure 2. Design principle of induction coils for sheet metal heating [18, 42]

Currently, induction heating is mainly applied for melting and forging processes and heat treatment operations [11, 42]. Multiple research efforts have been made to enable its application for sheet metal heating during the press hardening process [18, 21, 22, 28, 37, 42]. All of those investigations show the potential of inductive heating. However, they also indicate problems with the temperature distribution in inductively heated sheets [28] or secondary heating through convection and radiation or contact to achieve homogeneous temperatures [21, 22, 37].

In [29], a process was developed utilising a standalone longitudinal field inductor for homogeneous heating of complexly formed sheet geometries. Materials used were 22MnB5 and 20MnB8 with Al-Si, Zn-Fe and Nano-particle coatings. The upper part of a B-pillar was

heated to 950 °C for 16 s employing inductive heating. The homogeneity of temperature and material properties, comparable to the conventional furnace process, could be achieved. Since that process allows press hardening of structures comparable to realistic geometries of press-hardened parts entirely based on induction, it is used as a baseline for this investigation. While the applicability of the heating concept could be proven from a material and process perspective, no data are available regarding the economic and ecological feasibility of such an induction process.

METHODOLOGICAL APPROACH

The objective of the current study is to estimate GHG emissions and energy costs caused by inductive heating during the use phase of an inductive heating unit and compare the results with data from conventional gas-fired conveyor furnaces. Specific energy demands for induction and furnace heating are determined to achieve this goal. These serve as input for a model predicting emissions and energy costs of press hardening heating units considering various boundary conditions, such as good-mass flow and operating state, and different energy system transition scenarios. The results are subsequently used to determine possible break-even points of GHG emissions and inductive heating costs.

Modelling of specific energy demand

The specific energy demand of the fossil-fired roller hearth furnace as the comparison reference is modelled by a regression model based on the measuring data described in the work of Meuser [19]. The material heated in the examined roller hearth furnaces is the commonly used boron-manganese steel 22MnB5 with Al-Si coating. The operating states, production and standby characterise the production-technical framework conditions. While the energy demand during production is linearly dependent on the material mass flow, the energy demand during standby is described almost constantly by the heat losses through exhaust gas and furnace surfaces. Standby depends on planned disturbances like set-up times, tool changes and maintenance, and unplanned disturbances like transport, handling or pressing system errors. A linear regression model is derived for the furnace under investigation, yielding the natural gas input \dot{V}_{ng} [m³/h] as a function of the material mass flow \dot{m} [kg/s] with a standby of 24.3 m³/h and a coefficient of determination $R^2 = 0.982$:

$$\dot{V}_{ng} = 92.9 \times \dot{m} + 24.3 \quad (1)$$

On this basis, one can draw up a matrix of specific energy demands for different utilisation rates u and good-mass flows \dot{m} . For this purpose, the natural gas volume flow must be converted to the specific energy demand using the calorific value of 10.14 kWh/m³. The energy demand in kWh of a roller hearth furnace over a defined operating time t can be calculated using the following formula where the limits of integration are from 0 to t :

$$E_{tot} = 10.14 \times \int (\dot{V}_{ng} \times u + 24.3 \times (1 - u)) \times dt \quad (2)$$

The specific energy demand in kWh/kg as a function of the good-mass flow \dot{m} can then be calculated using the following:

$$e_f = \frac{E_{tot}}{m} = \frac{10.14 \times [\dot{V}_{ng} \times u + 24.3 \times (1 - u)]}{\dot{m}} \quad (3)$$

where m denotes the mass of the sheet metal heated in the time interval t . The specific energy demand for inductive heating can be derived from the data provided in [29]. Thermal energy

needed for sheet metal heating E_{sh} is calculated based on temperature-time-data for inductive heating using Equation (4):

$$dE_{sh} = m \times c_{p,22MnB5}(T) \times dT \quad (4)$$

Temperature-sensitive values for the specific heat capacity of 22MnB5 $c_{p,22MnB5}$ are drawn from the work of Vibrans [18]. The efficiency factor of the induction system used in [29] has been determined through measurements. For heating the upper B-pillar sheet, the efficiency factor η_{preC} is 0.72 for temperatures below Curie temperature. Above Curie temperature, efficiency is reduced considerably due to increased magnetic permeability of the material, leading to an efficiency factor η_{postC} of 0.28. The total energy needed for the heating process E_{tot} can then be determined according to Equation (5), factoring in thermal losses due to radiation $E_{l,rad}$ and convection $E_{l,conv}$ as well as electric losses in the induction system $E_{l,el}$:

$$E_{tot} = \frac{E_{sh,preC}}{\eta_{preC}} + \frac{E_{sh,postC}}{\eta_{postC}} = E_{sh} + E_{l,rad} + E_{l,conv} + E_{l,el} \quad (5)$$

With:

$$E_{sh} = E_{sh,preC} + E_{sh,postC} \quad (6)$$

Since longitudinal field induction is not yet used in industrial press hardening processes, the energy behaviour of such a heating system needs to be modelled. The following assumptions were made to set the boundary conditions for the model:

1. The efficiency factors determined for the heating of upper B-pillar parts can be taken as a baseline for an industrial longitudinal field induction heating process.
2. In an industrial process one inductor geometry would be used to heat all available sheet metal geometries. This inductor would be designed and optimised for manufacturing the largest geometry.
3. The good-mass flow would only be controlled by the surface area of the sheet metal geometry. Therefore, sheet thickness and heating parameters would stay constant.

Under these conditions, E_{tot} in dependence on the good-mass flow can be estimated based on the thermic energy E_{sh} as well as the thermic losses due to radiation $E_{l,rad}$ and convection $E_{l,conv}$. All these quantities can be directly related to the area A of a sheet metal geometry:

$$dE_{sh} = \rho_{22MnB5} \times t_{sh} \times A \times c_{p,22MnB5}(T) \times dT \quad (7)$$

$$dE_{l,rad} = 2 \times A \times \varepsilon_{22MnB5} \times \sigma \times (T^4 - T_{\infty}^4) dt \quad (8)$$

$$dE_{l,conv} = 2 \times A \times \alpha(T) \times (T - T_{\infty}) dt \quad (9)$$

Temperature-sensitive values for the heat-transfer coefficient α and the emissivity coefficient for 22MnB5 steel ε_{22MnB5} were drawn from the work of Shapiro [43]. According to the assumptions made for inductive heating on an industrial scale, the surface area A of the sheet metal geometry depends on the good-mass flow. The target temperature for inductive heating is determined to be 950 °C and the ambient temperature T_{∞} is assumed to be 25 °C. The constant of proportionality σ is the Stefan-Boltzman constant, according to the Stefan-Boltzmann law. The appendix of this work presents an overview of the data used for this calculation.

While electric losses get influenced by sheet metal geometry, the impact of these variations on the total value of electric losses is minor. Therefore, they are considered constant for this

conservative estimation, which leads to slightly worse efficiency factors of inductive heating than expected in praxis. One can then describe the energy demand in kWh of the induction heating system for one sheet metal plate dependent on good-mass flow using the following formula:

$$E_{tot} = 0.66 \times \dot{m} + 0.22 \quad (10)$$

The resulting specific energy demand is defined as:

$$e_{ind} = \frac{E_{tot}}{m} \quad (11)$$

Where m is the mass of a sheet metal plate corresponding to the good-mass flow. Equation (11) represents the energy demand of inductive heating during production. Since, unlike roller hearth furnaces, induction-heating units require no time to be heated up, an inductive system can be shut down completely during standby, resulting in an energy demand of 0 kWh during that operating state.

Energy system transition scenarios

Various international studies have analysed the development of energy costs in Europe to estimate future energy prices. A conclusion, which can be drawn from those studies, is that fossil energy prices will increase overall. The decisive factor for the increase in fossil energy prices is an estimated increase in CO₂ costs in the future. The forecasts assume only slightly increased prices for raw materials such as coal and natural gas [44–54].

Some studies assume that the price of electricity will also rise in the future [44, 45, 54, 55]. Since electricity production still depends on fossil fuels, the price increase is partly due to the rising prices for fossil energy [45]. Another factor, however, is that one can expect electricity demand to increase in the future [52]. The increased demand is associated with higher investment costs for grid expansion and the expansion of generation capacities [44, 45, 51], to be reflected in the electricity prices. It is also assumed that expensive Power-to-Gas fuels will have to be used for the goal of climate neutrality. These could set the marginal costs in the future [44]. In the European reference scenario [49], on the other hand, it is assumed that prices for industrial customers will remain stable on average. The Danish Energy Agency makes a similar forecast until 2030 [53].

Based on the two forecasts, Rising and Stable scenarios are built up in the following. For this purpose, the current energy costs for various countries were considered [56]. One high- and one low-cost country was selected for industrial customers, as well as the average of the EU 27. Germany serves as a high-price example, and Sweden is a low-price example.

Estimates were made for the increase in wholesale prices $p_{el,a,w}$ in Germany based on the scenarios from Burstedde and Nicolosi [44]. The other price components p_{tax} , such as grid charges and non-refundable levies, were derived from [57]. This results in the price for industrial customers $p_{el,a,tot}$ until 2045:

$$p_{el,a,tot,G} = p_{el,a,w,G} + p_{tax} \quad (12)$$

In the scenarios for rising electricity prices, the price increase for the EU27 and Sweden was transferred according to the formula:

$$p_{el,a,tot} = p_{el,2020,tot} \times \frac{p_{el,a,tot,G}}{p_{el,2020,tot,G}} \quad (13)$$

The natural gas prices $p_{ng,a,tot}$ until 2040 were taken from the projections of Repenning *et al.* [46] and extended by CO₂ price $p_{CO_2,a}$ according to [58]. The emission coefficient f_{ng} of natural gas is assumed to be 202 gCO₂/kWh according to [59, 60]:

$$p_{ng,a,tot} = p_{ng,a,w} + f_{ng} \times p_{CO_2,a} \quad (14)$$

The development of natural gas prices in Sweden is calculated as described in [14]:

$$p_{ng,a,tot} = p_{ng,2020,w} \times \frac{p_{el,a,w,G}}{p_{el,2020,w,G}} + e_{gas} \times p_{CO_2,a} \quad (15)$$

Natural gas prices in the EU27 in 2020 are at a similar price level as in Germany. Therefore, the same development is assumed here.

The development of the German electricity mix emissions until 2040 is based on the projections of Repenning *et al.* [46]. For 2045, the target of net zero emissions is assumed, while the value for 2020 is based on estimates by Icha *et al.* [61]. The EU 27 electricity mix trends adjusted to that of the German electricity mix starting from the 2020 value [62]. Sweden's emissions from the electricity grid are already significantly lower than the EU27 [63]. The target for 2040 is to cover 100% of electricity production with renewables [64].

In addition to forecasting the energy prices and emissions, the gas to electricity prices ratio is determined according to eq. (16):

$$ratio_a = \frac{p_{el,a,tot}}{p_{ng,a,tot}} \quad (16)$$

The same logic is also applied to calculating the gas and electricity emissions ratio.

RESULTS

The presented method allows for describing the gas consumption of a roller hearth furnace and electrical energy demand per part of an inductive heating system as functions of the good-mass flow. Gas consumption ranges from 26.1 m³/h at a good-mass flow of 0.02 kg/s to 70.7 m³/h at a good-mass flow of 0.5 kg/s. The energy demand ranges from 0.23 kWh for a good-mass flow of 0.02 kg/s to 0.55 kWh at 0.5 kg/s. Electric losses of induction heating, as described by the applied model, have been determined at 0.22 kWh and verified through measurements of the energy demand of no-load induction for relevant system operating states during heating. The measurements indicate electric losses of 0.20 kWh, proving the employed model's accuracy for energy demand determination.

The specific energy demand in dependence on good-mass flow can be determined for varying operating state shares (production and standby), as shown in Figure 3. Since an induction heating system can be shut down during standby, operating states do not influence the specific energy demand. Even for manufacturing with no standby times, the specific energy demand for induction heating is slightly lower than that of the furnace heating process. Specific energy demand ranges from 0.35 kWh/kg at a good-mass flow of 0.5 kg/s to 3.46 kWh/kg at a good-mass flow of 0.02 kg/s for induction heating to 0.40 kWh/kg and 3.68 kWh/kg for the furnace process at respective good-mass flows. The difference increases with an increasing share of the standby operating state.

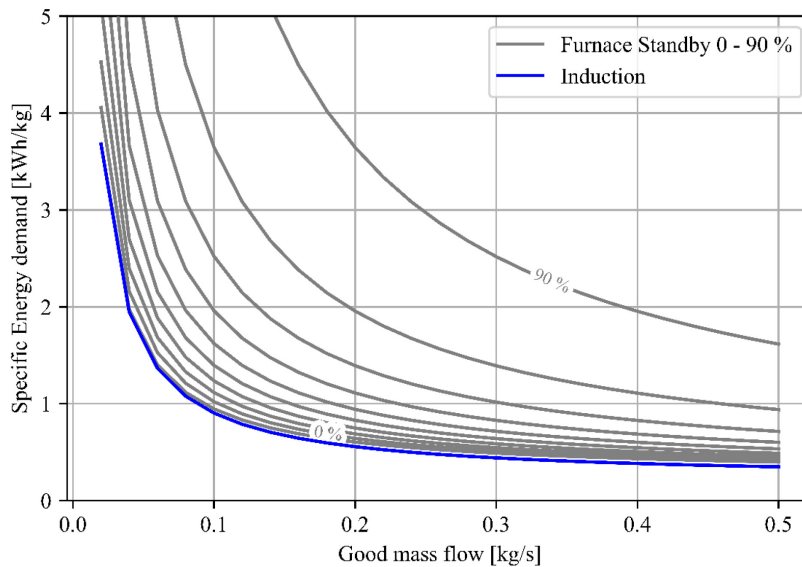


Figure 3. Specific energy demand of furnace and induction heating in dependence on good-mass flow and operating state

For the two price scenarios Rising and Stable, results for Germany, Sweden and the EU27 are shown in **Figure 4a**. The initial values in 2020 are taken from a data set of the Federal Ministry for Economic Affairs and Climate Action [60]. Gas prices are determined for consumers between 100,000 GJ and 1,000,000 GJ, and since prices for natural gas for Germany and the EU27 are close to each other, Germany is used as a reference (Germany/EU27: 2.32 ct/kWh, Sweden: 3.34 ct/kWh). Electricity prices are determined for consumers between 500 MWh and 2,000 MWh (Germany: 12.39 ct/kWh, EU27: 8.83 ct/kWh, Sweden: 4.88 ct/kWh). Both electricity and gas prices exclude VAT and recoverable taxes and levies.

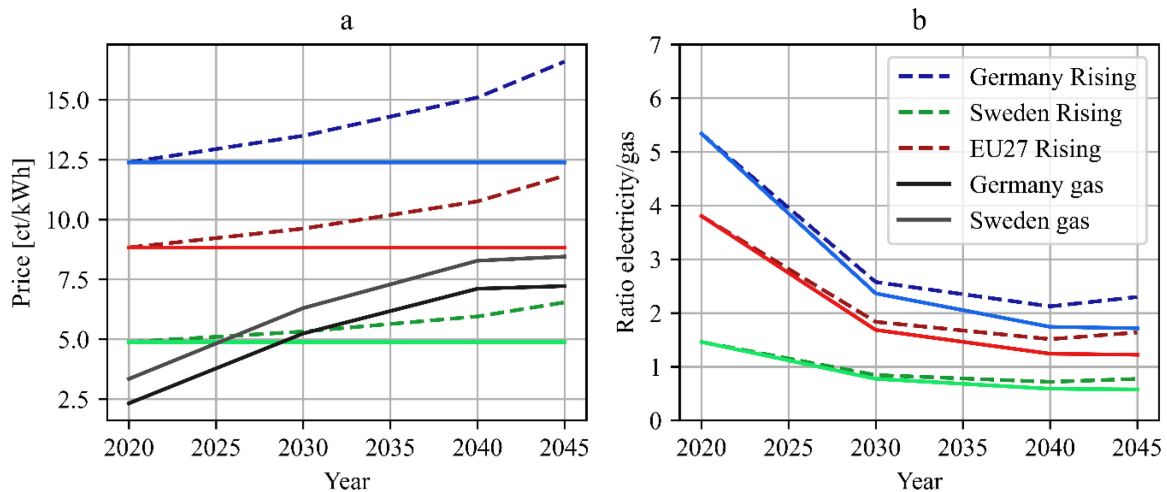


Figure 4. Evolution of gas and electricity prices (a) and the ratio of electricity to gas prices (b) until 2045

Figure 4b shows the corresponding ratios of electricity to gas prices. The ratio decreases particularly strongly between 2020 and 2030 due to the introduction and increase of CO₂ costs for natural gas. Between 2030 and 2040, the ratio decreases further for all cases and both price scenarios. From 2040 onwards, the electricity-to-gas price ratio decreases only in the Stable scenario, while it increases in the Rising scenario. The trends are due to no further CO₂ price increases and a lesser increase in the wholesale price of natural gas than electricity.

The development of CO₂ emissions for Germany, the EU27 and Sweden is shown in **Figure 5**. As with prices, Germany has the highest emissions, the EU27 form a middle case, and Sweden is well below the EU average.

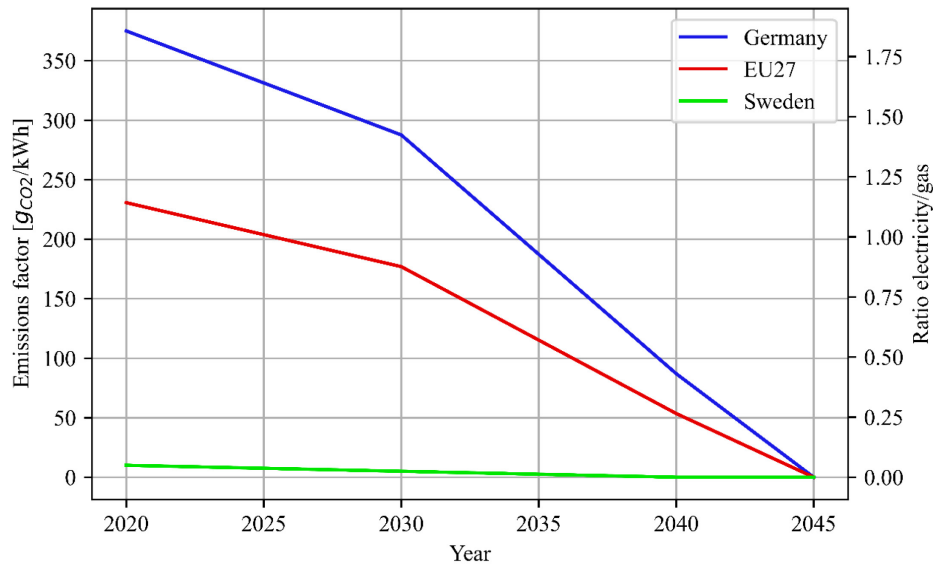


Figure 5. Evolution of energy grid emissions for Germany, the EU27 and Sweden until 2045

Energy cost

Due to the low electricity-to-gas price ratio in Sweden ($ratio_{SE,2020} = 1.46$), the specific energy costs for the use of induction heating are already lower than for the use of natural gas at a standby share of 50% and higher for all good flows in 2020, as shown in **Figure 6**. At a standby rate of 50%, cost savings of between 23% and 4% can be achieved, depending on the good-mass flow rate. From 2030 onwards, induction heating will provide a higher economic efficiency even with 100% occupancy of the roller hearth furnace. At full capacity utilisation and a material flow rate of 0.5 kg/s, the savings are greater than 34% in the scenario Rising and greater than 40% in the scenario Stable.

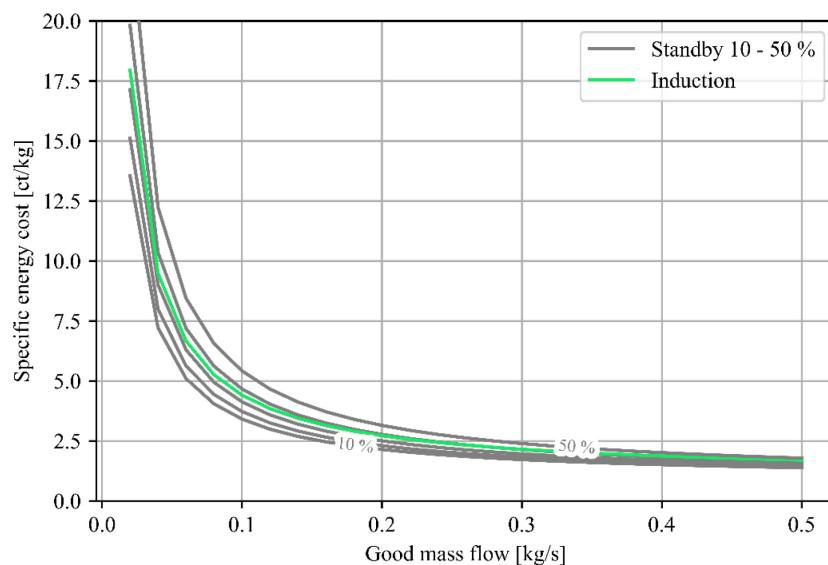


Figure 6. Specific energy costs for heating in Sweden 2020

In the price scenarios considered for Germany, cost savings can only be achieved depending on standby times, even in 2045. Specific energy costs for the year 2045 in Germany are shown in **Figure 7**. In the scenario Stable ($\text{ratio}_{G,2045,\text{Stable}} = 1.72$), savings of up to 27% can be achieved compared to a standby rate of 60%, depending on the good-mass flow. In the scenario Rising ($\text{ratio}_{G,2045,\text{Rising}} = 2.30$), savings of nearly 10% are possible with standby times of 70% and good-mass flows of 0.18 kg/s.

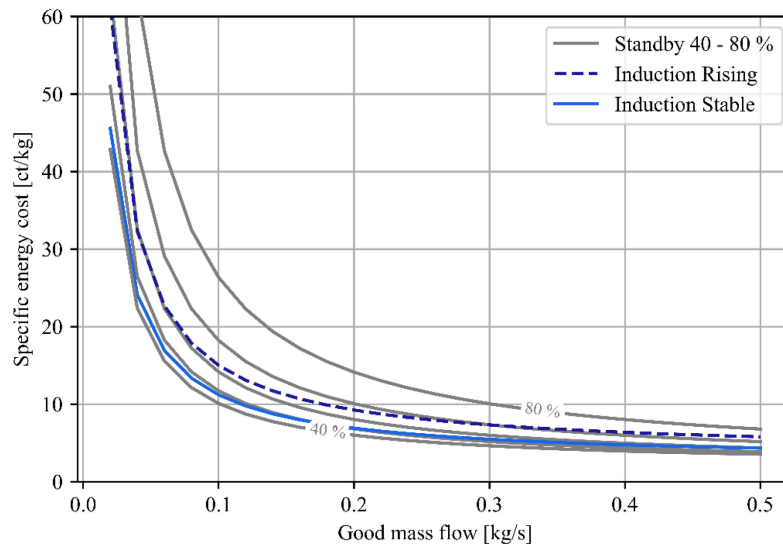


Figure 7. Specific energy costs for heating in Germany 2045

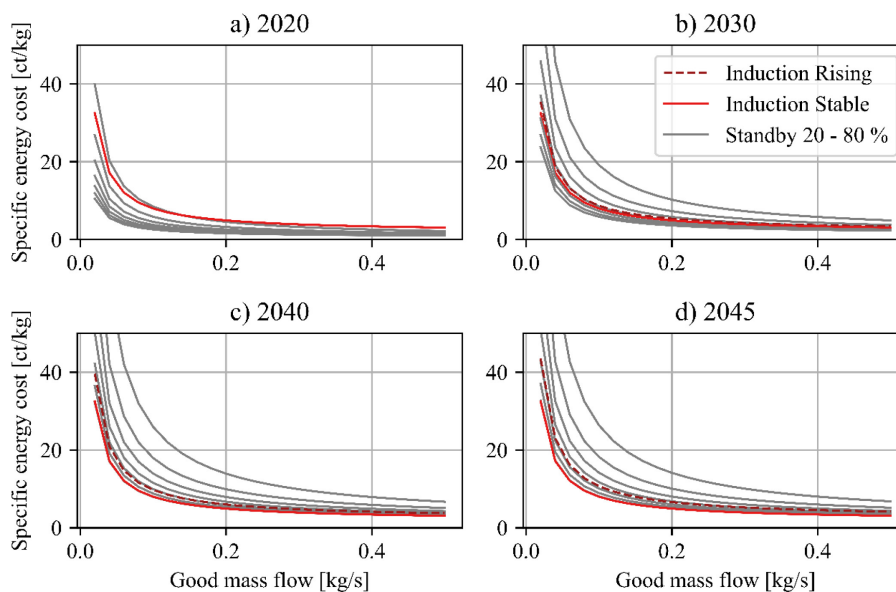


Figure 8. Specific energy costs for heating in the EU27 from 2020 (a) to 2045 (d)

Figures 8a to 8d show the development of specific energy costs for the EU27 in 2020, 2030, 2040 and 2045. While in 2020, costs can only be saved for systems with standby times above 80%, in 2030, inductive heating is also competitive with operating states at standby times of just under 70%. In the Stable scenario, cost savings of between 2% and 29% are possible compared to a roller hearth furnace with 60% standby times. In 2045, in the same scenario, electric heating would be more cost-effective at all good-mass flows than the fossil heating system with standby times of 20%. In the Rising scenario, induction heating would be competitive in 2045 compared to plants with downtimes of just under 60% for all good-mass flows.

Emission

Due to the low emission factor in the Swedish electricity grid, the CO₂ savings were already significant in 2020. The energy-related CO₂ emissions of the heating would decrease by over 96% for all good-mass flows. The emission savings decrease only slightly in 2030 before emissions reach zero in 2040 for the use of electrical energy.

On average, in the EU27, CO₂ savings would also have been possible as early as 2020. **Figure 9** shows that the curve of specific CO₂ emissions from 100% oven utilisation would have been lower using electrical energy via induction. Savings of between around 8% at a good-mass flow of 0.02 kg/s and almost 20% at a good-mass flow of 5 kg/s are the result. In 2030, the savings would be 30% to almost 40%; in 2040, savings would be greater than 80%.

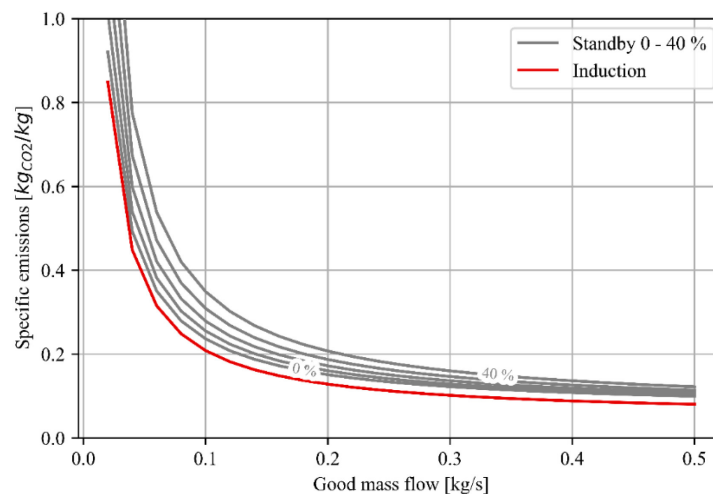


Figure 9. Specific emissions for heating in the EU 27 2020

In Germany, CO₂ savings between 40% and 50% were possible in 2020 compared to plants with standstill times, depending on the good-mass flow. In 2030, the savings compared to plants with 50% standby would be around 35% to 40%. Even in the case of furnaces with standby times of 10%, small CO₂ savings could be achieved with high material mass flows, as can also be seen in **Figure 10**. In 2040, the expected reduction in CO₂ emissions is between 65% and 70% before electric heating is CO₂-neutral in 2045.

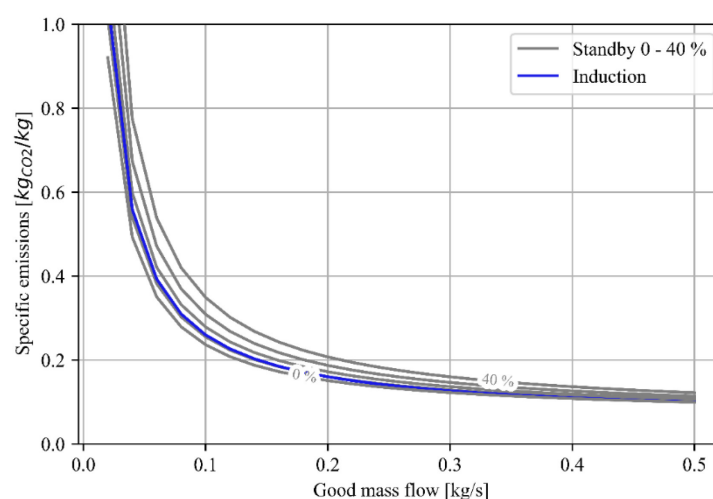


Figure 10. Specific emissions for heating in Germany 2030

DISCUSSION

While inductive heating seems generally more energy efficient than furnace heating, economic and ecological feasibility highly depends on regional pricing and emission factors of electric energy. It becomes apparent when comparing the different break-even scenarios for countries like Germany and Sweden. For Sweden, induction heating can provide lower specific emissions even today and lower specific prices independent of the operating state until 2030. In contrast, for Germany, the economic feasibility of induction heating still depends on the share of standby times during production in 2045. It is due to Germany's high electricity-to-gas price ratio, which affects induction heating and all electricity-based heating methods. It is, therefore, necessary to ensure a competitive electricity-to-gas price ratio to entice the use of alternative heating methods.

The results presented in this study provide a good first estimation of the potential of inductive heating for decarbonising the press hardening heating process. Since the results are based on scenarios and models estimating energy demand and future developments in the energy sector, one must consider uncertainties introduced by this approach. The forecasts used in this work provide a good foundation for evaluating future developments. However, recent events have shown that geopolitical incidents, such as pandemics or wars, can unexpectedly influence price evolution and energy system transition scenarios. For example, prices on the German power exchange (futures market) have increased fourfold compared to 2020 and are thus significantly above the highest estimate in the outlined scenarios [65]. At the same time, the price of natural gas in wholesale trading in Germany has increased fivefold from the beginning of 2021 until May 2022 and has temporarily increased more than tenfold [66]. It could be an indicator of electricity-to-gas price ratios improving faster than anticipated. While it is uncertain if this is a lasting effect or if future prices will normalise, it does emphasise the need to reduce dependence on fossil fuels. Nevertheless, this paper used country-specific price ratios for orientation purposes. The reader can also use the stated price ratios to assess company-specific or country-specific framework conditions.

In addition, assumptions and simplifications made for estimating the energy demand for inductive heating may influence the results. Efficiency factors and process parameters for inductive heating have been based on a prototype heating system. The scalability of such technology to an industrial standard still needs to be verified. The conversion of the prototype to a heating system matching industrial standards may also influence the system's thermic and electric efficiency, therefore impacting the overall efficiency factor of inductive heating. While assumptions regarding heating times and inductor geometries may hold for industrial processes depending on process and system structure, sheet metal thickness will likely vary based on the manufactured part. Depending on the sheet thickness and the frequency of the inductive heating system, this will negatively or positively influence energy efficiency.

The current study investigates the economic and ecological feasibility of induction heating based on heating energy demand. A transition from a press hardening manufacturing line with a furnace-based heating system to an induction-based heating system would have implications for the press hardening process reaching far beyond heating energy demand. Applying such a heating system requires optimising process planning, energy management and materials used for induction heating. It would also affect investment costs, space requirements and process flexibility – factors one must consider for a full economic and ecological feasibility assessment.

CONCLUSIONS

This work determined the specific energy demand for heating sheet metal plates for press hardening using a roller hearth furnace and induction heating based on a prototype induction unit. Various scenarios regarding the development of energy costs and energy grid emissions in Europe have been analysed. The results were used to identify ecological and economic

break-even points for applying inductive heating in various European countries with different energy transition scenarios. The following findings have been made:

1. Induction heating of sheet metal can be a valuable approach for reducing energy demand and GHG emissions of hardening press processes. In this study, the specific energy demand of inductive heating is lower than that of furnace heating, independent of the share of operating states.
2. In a scenario with 0% standby times, induction heating can save up to 12% energy compared to furnace heating. These savings increase with increasing standby times. At 20% standby operating state, energy savings of induction heating increase to up to 19%.
3. The ecological feasibility is highly dependent on the emission factors of the energy grid. GHG emissions reduction between 8% and 20% would have been possible for the EU27 even in 2020. For countries with a high share of renewable energy, like Sweden, savings would be even more significant. For countries with a high emission factor, like Germany, a share of the standby operating state is necessary for ecological feasibility. A standby share of 50% would be required in 2020, while in 2030, a share of 20% would be sufficient. Unconditional ecological feasibility for Germany is possible in 2040.
4. The economic feasibility depends on the electricity-to-gas price ratio. Countries with a low ratio will profit earlier from implementing induction heating for press hardening processes. In Sweden ($\text{ratio}_{\text{SE},2030} = 0.77\text{--}0.84$), economic feasibility can be reached in 2030, independent of the operating states of the heating system. For Germany ($\text{ratio}_{\text{SE},2045} = 1.72\text{--}2.30$), standby shares of 60% to 70% would be necessary even in 2045 for the economic feasibility of induction heating. A competitive electricity-to-gas price ratio is needed to entice the use of alternative heating methods.

To verify assumptions made in this study and for a holistic assessment of the economic and ecological impact of an inductive press hardening line, the investigated inductive heating system needs to be advanced to a standard of industrial series production. Such a development requires changes to the heating system of a press hardening line and optimisation of preceding and subsequent processes, production, and energy management, as well as materials and coatings for inductive heating.

ACKNOWLEDGMENT

The authors acknowledge the work and support of the Forschungsvereinigung Stahlanwendung e.V. (FOSTA), the Forschungsvereinigung Automobiltechnik (FAT), the Ministry of Economic Affairs, Industry, Climate Action and Energy of the state of North Rhine-Westphalia (MWIKE NRW), the Projektträger Jülich (PtJ) as well as a board of industry representatives.

NOMENCLATURE

Symbols

α	Heat transfer coefficient	[W/m ² K]
ε	Emissivity coefficient	[-]
η	Efficiency factor	[-]
ρ	Density	[kg/m ³]
σ	Boltzmann constant	[W/m ² K ⁴]
A	Surface area	[m ²]
c	Heat capacity	[J/kgK]
E	Energy	[kWh]
e	Specific energy	[kWh/kg]
f	Emission coefficient	[g _{CO2} /kWh]
m	Mass	[kg]
\dot{m}	Mass flow	[kg/s]
p	Price	[ct.]

T	Temperature	[K]
t	Thickness	[m]
u	Utilisation rate	[-]
\dot{V}	Volume flow	[m ³ /h]

Subscripts

∞	Environmental
2020	In the year 2020
22MnB5	For 22MnB5 steel
a	Year
CO ₂	Carbon dioxide
conv	Convection
el	Electric
em	Emission
EU	Europa
f	Furnace
G	Germany
ind	Induction
l	loss
ng	Natural gas
p	Constant pressure
preC	Pre Curie temperature
postC	Post Curie temperature
rad	Radiation
sh	Sheet
SWE	Sweden
tax	Other price components
tot	Total
w	Wholesale

Abbreviations

GHG	Greenhouse gas
-----	----------------

REFERENCES

1. European Union: European Commission, Report from the Commission to the European Parliament, the Council, the European Economic and Social Committee and the Committee of the Regions: State of the Energy Union 2021 – Contributing to the European Green Deal and the Union's Recovery, Report, 52021DC0950, Brussels, Belgium, 2021.
2. European Union: European Commission, Communication from the Commission to the European Parliament, the Council, the European Economic and Social Committee and the Committee of the Regions: A European Strategy for Low-Emission Mobility, Report, 52016DC0501, Brussels, Belgium, 2016.
3. European Environment Agency, EEA greenhouse gases: Sector shares in EU-27 in 2019, <https://www.eea.europa.eu/data-and-maps/data/data-viewers/greenhouse-gases-viewer> [Accessed: 25-05-2022].
4. Adamson, K.-M. et al., High-temperature and transcritical heat pump cycles and advancements: A review, *Renewable and Sustainable Energy Reviews*, vol. 167, p. 112798, 2022, <https://doi.org/10.1016/j.rser.2022.112798>.
5. Schlosser, F. et al., Large-scale heat pumps: Applications, performance, economic feasibility and industrial integration, *Renewable and Sustainable Energy Reviews*, vol. 133, p. 110219, 2020, <https://doi.org/10.1016/j.rser.2020.110219>.
6. Knorr, L., Schlosser, F., and Meschede, H., Assessment of Energy Efficiency and Flexibility Measures in Electrified Process Heat Generation Based on Simulations in the

- Animal Feed Industry, *J.sustain. dev. energy water environ. syst.*, vol. 11, no. 3, <https://doi.org/10.13044/j.sdewes.d11.0444>.
7. Schüwer, D. and Schneider, C., Electrification of industrial process heat: long-term applications, potentials and impacts, in: *ecee Industrial Summer Study proceedings* (T. Laitinen Lindström, ed.), pp. 411–422, Stockholm, Sweden, 2018.
 8. Redelbach, M., Klötzke, M., and Friedrich, H. E., Impact of lightweight design on energy consumption and cost effectiveness of alternative powertrain concepts, *Proceedings European Electric Vehicle Conference*, Brussels, Belgium, pp. 1–9, November 19–22, 2012.
 9. Shaffer, B., Auffhammer, M., and Samaras, C., Make electric vehicles lighter to maximize climate and safety benefits, *Nature*, vol. 598, no. 7880, pp. 254–256, 2021, <https://doi.org/10.1038/d41586-021-02760-8>.
 10. Wolfram, P. et al., Material efficiency and climate change mitigation of passenger vehicles, *Journal of Industrial Ecology*, vol. 25, no. 2, pp. 494–510, 2021, <https://doi.org/10.1111/jiec.13067>.
 11. Mori, K. et al., Hot stamping of ultra-high strength steel parts, *CIRP Annals*, vol. 66, no. 2, pp. 755–777, 2017, <https://doi.org/10.1016/j.cirp.2017.05.007>.
 12. Feuser, P. S., An approach to the manufacturing of press hardened car body components with tailored mechanical properties (in German), Meisenbach, Bamberg, 2012.
 13. Berglund, G., The history of hardening of boron steels in northern Sweden, in: *Proceedings of the 1st International Conference on Hot Sheet Metal Forming Of High-Performance Steel* (K. Steinhoff, M. Oldenburg, and B. Prakash, eds.), pp. 175–177, Bad Harzburg, Germany, 2008.
 14. Karbasian, H. and Tekkaya, A. E., A review on hot stamping, *Journal of Materials Processing Technology*, vol. 210, no. 15, pp. 2103–2118, 2010, <https://doi.org/10.1016/j.jmatprotec.2010.07.019>.
 15. Palm, C. et al., Increasing performance of Hot Stamping systems, *Procedia Engineering*, vol. 207, pp. 765–770, 2017, <https://doi.org/10.1016/j.proeng.2017.10.826>.
 16. Sjölin, U., Holmér, C., and Orsbeck, C., The All-New V60 2018 Car Body, Bad Nauheim, 16.10.2018, 2018, [https://doi.org/10.1016/S1350-4789\(18\)30104-1](https://doi.org/10.1016/S1350-4789(18)30104-1).
 17. Zeichner, A., Development of a furnace roll coating for press hardening (in German), Dissertation, RWTHA Inst. Mining Eng., Aachen, Germany, 2013.
 18. Vibrans, T., Inductive heating of formed plates for warm forming (in German), Dissertation, TUC IWP, Chemnitz, Germany, 2016.
 19. Meuser, J., Waste heat potential of industrial furnaces (in German), Dissertation, University Kassel upp, Kassel, Germany, 2019.
 20. Veit, R. and Kolleck, R., Current and Future Trends in the field of Hot Stamping of Car Body Parts, in: *3rd International Conference on Steels in Cars and Trucks: Future trends in steel development, processing technologies and applications* (H. J. Wieland, ed.), pp. 67–74, Düsseldorf, Germany, 2011.
 21. Opitz, T. and Vibrans, T., Fast Induction Heating for Press Hardening of Shaped Blanks in Automotive Production, *Journal of Heat Treatment and Materials*, vol. 6, no. 70, pp. 261–266, 2015, <https://doi.org/10.3139/105.110270>.
 22. Veit, R. et al., Development of a Close-to-production Prototype of an Induction Heating Device for Hot Stamping of Boron Alloyed Steels, in: *3rd International Conference on Steels in Cars and Trucks: Future trends in steel development, processing technologies and applications* (H. J. Wieland, ed.), pp. 83–90, Düsseldorf, Germany, 2011.
 23. DIN Deutsches Institut für Normung e.V., Manufacturing processes: Terms and definitions, DIN 8580, Berlin, 2020.
 24. Naderi, M., Hot Stamping of Ultra High Strength Steels: Presshärten ultrahochfester Stähle, Dissertation, Lehrstuhl und Institut für Eisenhüttenkunde, RWTH Aachen, Aachen, 2008.

25. thyssenkrupp AG, MBW: Product information for manganese-boron steels for hot forming, https://www.thyssenkrupp-steel.com/media/content_1/publikationen/produktinformationen/mbw/thyssenkrupp_mbw_product_information_steel_en.pdf [Accessed: 27-05-2022].
26. Lee, E.-H. et al., A local heating method by near-infrared rays for forming of non-quenched advanced high-strength steels, *Journal of Materials Processing Technology*, vol. 214, no. 4, pp. 784–793, 2014, <https://doi.org/10.1016/j.jmatprotec.2013.11.023>.
27. Shimizu, J. et al., Low-Cost Hot Stamping Method by Far-Infrared Ray Heating Technique, Technical Report, 11A1106501, Tokyo, Japan, 2016.
28. Tröster, T. and Niewel, J., Application of inductive heating for sheet metal and determination of appropriate process window for press hardening (in German), Düsseldorf: Verl. und Vertriebsges. mbH, Düsseldorf, 2014.
29. Tröster, T. et al., Series-production of inductively heated blanks for hot sheet metal forming (in German), Düsseldorf: Verl. und Vertriebsges. mbH, Düsseldorf, 2021.
30. Mori, K., Maki, S., and Tanaka, Y., Warm and Hot Stamping of Ultra High Tensile Strength Steel Sheets Using Resistance Heating, *CIRP Annals*, vol. 54, no. 1, pp. 209–212, 2005, [https://doi.org/10.1016/S0007-8506\(07\)60085-7](https://doi.org/10.1016/S0007-8506(07)60085-7).
31. Maeno, T. et al., Full Hardening of Products in Hot Stamping Using Rapid Resistance Heating, in: *Proceedings of the 5th International Conference on Hot Sheet Metal Forming Of High-Performance Steel* (K. Steinhoff, M. Oldenburg, and B. Prakash, eds.), pp. 323–330, Bad Harzburg, Germany, 2015.
32. Mori, K., Smart Hot Stamping for Ultra-high Strength Steel Parts, in: *60 Excellent Inventions in Metal Forming* (A. E. Tekkaya, ed.), pp. 403–408, Berlin/Heidelberg, Germany, 2015, https://doi.org/10.1007/978-3-662-46312-3_62.
33. Behrens, B.-A. et al., Conductive Heating Opens up Various New Opportunities in Hot Stamping, in: *Reports from the IWU*, vol. 88, *Proceedings of the 5th International Conference on Accuracy in Forming Technology* (D. Landgrebe, W.-G. Drossel, and M. Putz, eds.), pp. 157–173, Auerbach, Germany, 2015.
34. Ploshikhin, V. et al., New heating technology for the furnace-free press hardening process, *Proceedings of Tools and Technologies for Processing Ultra High Strength Materials*, Graz, Austria, pp. 1–8, September 19-21, 2011.
35. Andreiev, A., Grydin, O., and Schaper, M., A Rapid Heating Method for Press Hardening Processing, in: *The Minerals, Metals & Materials Series, Proceedings of the 3rd Pan American Materials Congress* (M. A. Meyers et al., eds.), pp. 723–736, Heidelberg, Germany, 2017, https://doi.org/10.1007/978-3-319-52132-9_72.
36. Landgrebe, D. et al., Towards Efficient, Interconnected and Flexible Value Chains – Examples and Innovations from Research on Production Technologies, in: *Reports from the IWU*, vol. 88, *Proceedings of the 5th International Conference on Accuracy in Forming Technology* (D. Landgrebe, W.-G. Drossel, and M. Putz, eds.), pp. 61–78, Auerbach, Germany, 2015.
37. Kim, D. K. et al., Advanced induction heating system for hot stamping, *Int J Adv Manuf Technol*, vol. 99, 1-4, pp. 583–593, 2018, <https://doi.org/10.1007/s00170-018-2385-z>.
38. Tröster, T. et al., Fluidised bed heating of blanks for press hardening (in German), Düsseldorf: Verl. und Vertriebsges. mbH, Düsseldorf, 2010.
39. Bors, M., Paceflame - A Versatile Tool to Boost Efficiency in Hot Forming Processes, in: *Proceedings of the 5th International Conference on Hot Sheet Metal Forming Of High-Performance Steel* (K. Steinhoff, M. Oldenburg, and B. Prakash, eds.), pp. 315–322, Bad Harzburg, Germany, 2015.
40. Veit, R. et al., Phase Formation of Al/Si-Coatings during Induction Heating of Boron Alloyed Steel Sheets, *Proceedings of Tools and Technologies for Processing Ultra High Strength Materials*, Graz, Austria, pp. 225–233, September 19-21, 2011, <https://doi.org/10.1063/1.3552543>.

41. Todzy, T., Process window during press hardening with rapid heating of steel blanks with aluminium-silicon coating (in German), Shaker-Verlag, Aachen, 2015.
42. Kolleck, R. et al., Investigation on induction heating for hot stamping of boron alloyed steels, *CIRP Annals*, vol. 58, no. 1, pp. 275–278, 2009, <https://doi.org/10.1016/j.cirp.2009.03.090>.
43. Shapiro, A. B., Using LS-Dyna for Hot Stamping, Proceedings of the 7th European LS-DYNA Conference, Salzburg, Austria, pp. 1–9, May 14-15, 2009.
44. Burstedde, B. and Nicolosi, M., Electricity market and climate protection: transforming electricity generation by 2050 (in German), Report, FB000406, Dessau-Roßlau, Germany, 2021.
45. Riechmann, C. et al., Impact assessment of the CO2 sector target for the energy industry in the Climate Protection Plan 2050 (in German), Report, Essen, Germany, 2018.
46. Repenning, J. et al., Projection Report 2021 for Germany (in German), Report, 282715, Berlin, Germany, 2021.
47. Kreidelmeyer, S. et al., Costs and transformation pathways for electricity-based energy sources (in German), Studie im Auftrag des Bundesministeriums für Wirtschaft, Report, Basel, Switzerland, 2020.
48. Schlesinger, M. et al., Development of the energy markets: Energy reference forecast (in German), Report, Berlin, Germany, 2014.
49. European Union: European Commission, EU Reference Scenario 2020: Energy, transport and GHG emissions - Trends to 2050, Report, Brussels, Belgium, 2021.
50. IEA, World Energy Outlook 2021, Report, Paris, France, 2021.
51. IEA, World Energy Outlook 2020, Report, Paris, France, 2020.
52. IEA, Net Zero by 2050, Report, Paris, France, 2021.
53. Danish Energy Agency, Denmark's Energy and Climate Outlook 2019, Report, Copenhagen, Denmark, 2019.
54. Ministry of the Environment and Energy, Ed., Sweden's draft integrated national energy and climate plan, Report, Stockholm, Sweden, 2020.
55. Mier, M. et al., Costs and Benefits of Political and Physical Collaboration in the European Power Market, Report, No. 343, Munich, Germany, 2020.
56. BMWK, Facts and figures: Energy data: National and international development (in German), Report, Berlin, Germany, 2022.
57. BDEW, Electricity price analysis January 2022 (in German), Report, Berlin, Germany, 2022.
58. Kemmler, A. et al., Energy projections and impact assessments 2030/2050 (in German), Report, Basel, Switzerland, 2020.
59. Juhrich, K., CO2 Emission Factors for Fossil Fuels, Report, Climate Change | 29/2022, Dessau-Roßlau, Germany, 2016.
60. Zijlema, P. J., The Netherlands: list of fuels and standard CO2 emission factors version of January 2020, Report, The Hague, Netherlands, 2020.
61. Icha, P., Lauf, T., and Kuhs, G., Development of the specific carbon dioxide emissions of the German electricity mix in the years 1990 - 2020 (in German), Report, Climate Change | 45/2021, Dessau Roßlau, Germany, 2021.
62. European Environment Agency, Greenhouse gas emission intensity of electricity generation, <https://www.eea.europa.eu/data-and-maps/indicators/overview-of-the-electricity-production-3/assessment-1> [Accessed: 25-05-2022].
63. Statista, Carbon intensity of the power sector in Sweden from 2000 to 2021, <https://www.statista.com/statistics/1290491/carbon-intensity-power-sector-sweden/> [Accessed: 10-06-2022].
64. Swedish Institute, Energy use in Sweden, <https://sweden.se/climate/sustainability/energy-use-in-sweden> [Accessed: 10-06-2022].

65. BDEW, Electricity price analysis April 2022 (in German), Report, Berlin, Germany, 2022.
66. BDEW, Gas price analysis April 2022 (in German), Report, Berlin, Germany, 2022.

APPENDIX

Table 1. Temperature sensitive values for the heat-transfer coefficient according to Shapiro [43]

Temperature [°C]	α [W/m ² °C]
50	5.68
100	6.80
200	7.80
300	8.23
400	8.43
500	8.51
600	8.52
700	8.50
800	8.46
900	8.39
1000	8.32

Table 2. Temperature-sensitive values for the specific heat capacity of 22MnB5 according to Vibrans [18]

Temperature [K]	Specific heat capacity 22MnB5 [kJ/kg K]
299.75	593
322.45	504
372.35	510
421.65	524
473.15	539
523.55	556
573.55	569
623.35	584
673.15	597
723.15	618
773.05	644
822.95	675
872.95	710
922.85	748
972.85	879
992.65	941
1012.65	969
1032.65	1036
1052.65	864
1072.65	836
1092.65	826
1132.65	836
1152.65	843
1172.65	848
1222.65	852
1272.55	896

Table 3. Surface area of the sheet metal geometry in dependence on the good-mass flow

Good-mass flow [kg/s]	Surface area [m ²]
0.00	0.00
0.02	0.03
0.04	0.05
0.06	0.08
0.08	0.11
0.10	0.14
0.12	0.16
0.14	0.19
0.16	0.22
0.18	0.24
0.20	0.27
0.22	0.30
0.24	0.33
0.26	0.35
0.28	0.38
0.30	0.41
0.32	0.43
0.34	0.46
0,36	0.49
0.38	0.52
0.40	0.54
0.42	0.57
0.44	0.60
0.46	0.63
0.48	0.65
0.50	0.68

Table 4. Constant parameters used for calculation of inductive energy demand

Emissivity coefficient 22MnB5 [-]	Stefan-Boltzmann constant [W/m ² K ⁴]	Target temperature [°C]	Ambient temperature [°C]
0.80	$5.670374419 \times 10^{-8}$	950	25



Paper submitted: 08.01.2023
 Paper revised: 02.04.2023
 Paper accepted: 08.04.2023